INVESTIGATION AND CONSTRUCTION OF SELF-OSCILLATING

SYSTEMS

A Thesis

by

GUANQUN WANG

Submitted to the Office of Graduate Studies of
Texas A&M University
in partial fulfillment of the requirements for the degree of

MASTER OF SCIENCE

May 2010

Major Subject: Materials Science and Engineering

INVESTIGATION AND CONSTRUCTION OF SELF-OSCILLATING

SYSTEMS

A Thesis

by

GUANQUN WANG

Submitted to the Office of Graduate Studies of
Texas A&M University
in partial fulfillment of the requirements for the degree of

MASTER OF SCIENCE

Approved by:

Chair of Committee,   Zhengdong Cheng
Committee Members,   Abraham Clearfield
    Hung-Jue Sue
Intercollegiate
Faculty Chair,   Ibrahim Karaman

May 2010

Major Subject: Materials Science and Engineering

ABSTRACT

Investigation and Construction of Self-oscillating Systems. (May 2010)

Guanqun Wang, B.S., University of Science and Technology of China

Chair of Advisory Committee: Dr. Zhengdong Cheng

Self-oscillating reactions have been widely observed and studied since the last century because they exhibit unique behaviors different from the traditional chemical reactions. Self-oscillating systems, such as the Belousov-Zhabotinsky (BZ) reaction, oxidation reaction of CO on single crystal Pt, and calcium waves in the heart tissue, are of great interest in a variety of scientific areas. This thesis contributes to the understanding of wave transition in BZ reaction, and to possible applications of non-equilibrium behaviors of polymer systems.

In BZ reaction, two types of wave patterns, target and spiral, are frequently observed. The transition from one to another is not fully understood. Hence, a systematic investigation has been performed here to investigate the mechanism by which heterogeneity affects the formation of wave patterns. A BZ reaction catalyst was immobilized in ion exchange polystyrene beads to form active beads. Then active and inactive beads with no catalyst loading were mixed together with various ratios to achieve various levels of heterogeneity. In the same reaction environment, different wave patterns were displayed for the bead mixtures. We observed a transition from target patterns to spiral patterns as the percentage of the active beads in the beads

mixture decreased. The increase of the heterogeneity led to wave pattern transition. Heterogeneity hindered the propagation of target waves and broke them into wavelets that generated spiral waves.

In an effort to develop practical applications based on non-equilibrium phenomena, we have established a novel drug delivery system. A proton generator Zirconium Phosphate (ZrP) was imbedded inside a pH sensitive polymer matrix, poly acrylic acid (PAA). Through the ion exchange with sodium cation (Na^+), ZrP generates protons to control the swelling/shrinking behaviors of PAA. The drug encapsulated in the matrix can be released in a controlled manner by adjusting the supply of Na^+. This system might be developed into vehicles to deliver drugs to specific targets and release at a proper time. This new delivery technique will be convenient and significantly increase the efficiency of medicines.

To my parents, my wife and my friends.

ACKNOWLEDGEMENTS

Thanks to my committee chair, Dr. Zhengdong Cheng, for his unending guidance, support and encouragement in completing this thesis. I would also like to thank committee members, Dr. Abraham Clearfield and Dr. Hung-Jue Sue, for their advice and encouragement throughout the research.

Thanks also go to my friends and colleagues and the department faculty and staff for making my time at Texas A&M University a great experience.

Finally, thanks to my parents and my wife for their encouragement, support and love.

TABLE OF CONTENTS

LIST OF FIGURES

CHAPTER I

INTRODUCTION

Studies on Heterogeneous Self-Oscillating Systems

Self-oscillating systems have been studied for a long time since its discovery by Bray in 1921[1]. Based on the dual role of hydrogen peroxide as both oxidizing agent and a reducing agent, Bray developed the first typical self-oscillating model by mixing proper amount of hydrogen peroxide, potassium iodate and sulfuric acid together to set up a chemical system which could continuously switch between iodic acid and iodine. This self-oscillating system was unaccepted by most of the scientists at that time because it seemed to break the second law of thermodynamics. Later in 1958, Belousov developed another similar self-oscillating system which is the oxidation of citric acid catalyzed by cerium[2]. His student Zhabotinsky further developed the reaction by substituting ferroin for cerium and malonic acid for citric acid[3]. Thus, the classical self-oscillating system was finally established and accepted by the academic world. The result was an oscillatory reaction with striking color changes shown in Figure 1.1, which is now known as the Belousov–Zhabotinsky (BZ) reaction. By leaving in a stationary environment, the color change appeared to be continuous and wave patterns were generated. Target patterns[4] were first observed as shown in Figure 1.2. Later, by changing the concentration of the catalyst and the reactants and manually braking the target patterns, a new type wave pattern[5] was observed as shown in Figure 1.3. Instead

_____

This thesis follows the style of *Nature*.

of a closed circle, the new wave pattern expanded under the leading of the tip and rotated continuously. It is named spiral waves.
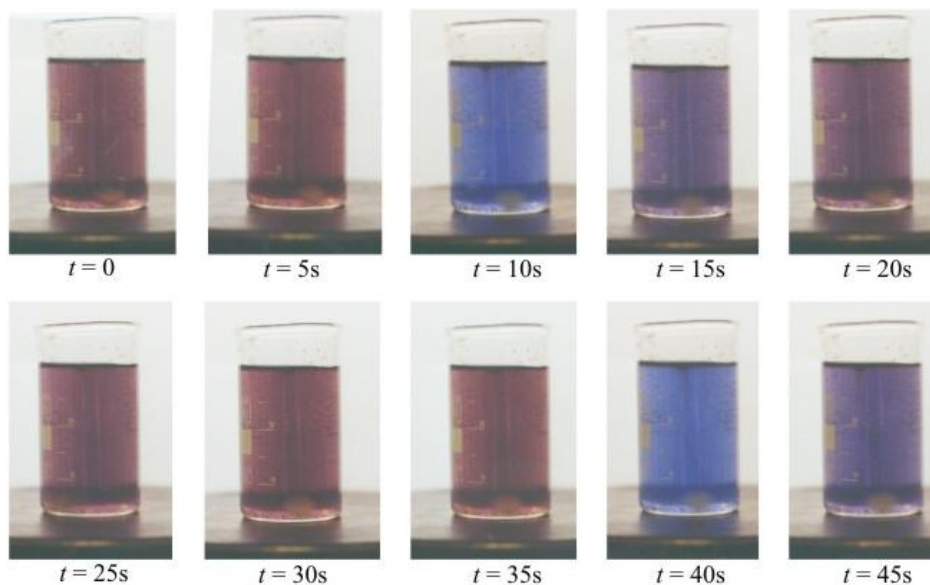
Figure 1.1 A stirred BZ reaction mixture showing color changes over time.
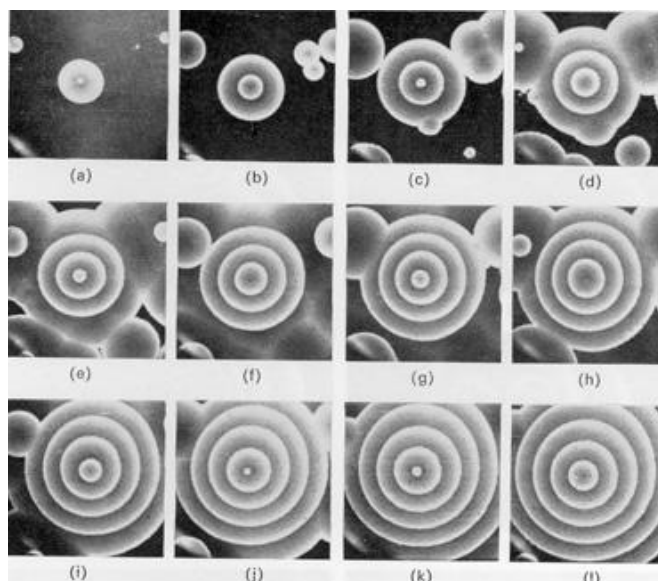
Figure 1.2 Generation of target pattern in the BZ reaction.[4]
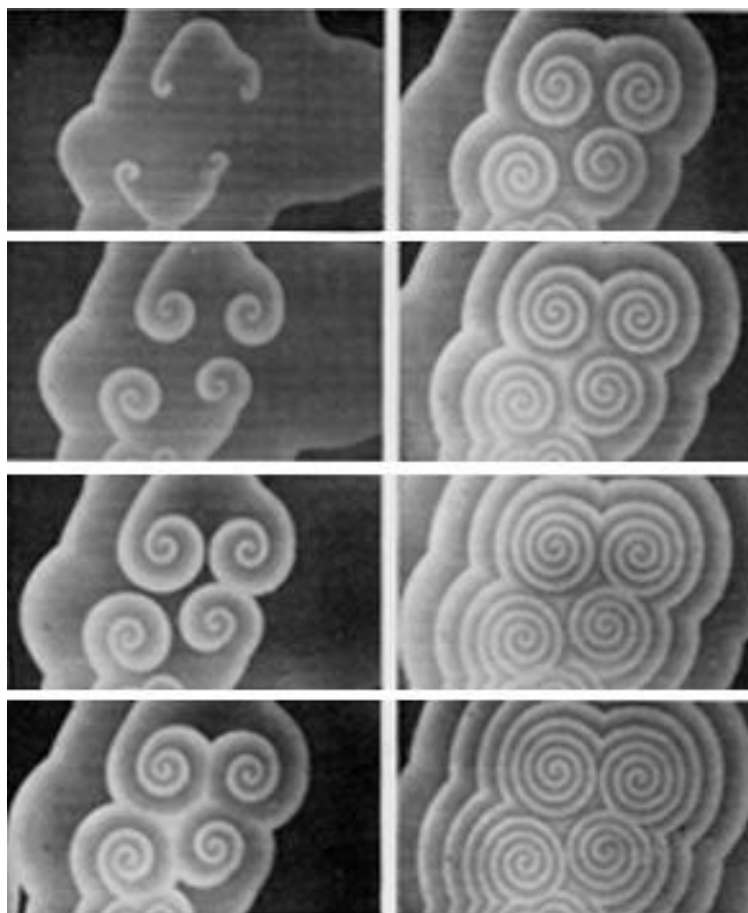
Figure 1.3 Development of spiral waves in the BZ reaction.[5]

Then scientists have developed various models[6-9] to study the mechanism of how the waves were generated and propagated. Since homogeneous environment is hard to achieve in the real world, recent research interested in the impact of heterogeneous factors on the formation and propagation of wave patterns was pursued. Scientists introduce heterogeneities by immobilizing the BZ catalyst in resin beads and feeding the reactant at various concentrations. Then spiral and target waves appeared spontaneously in the BZ reaction[10-11]. Later on, some similar waves were also observed in biological

excitable media, such as heart tissue [7,12-14]. The waves also have similar characteristics and wave pattern transition phenomenon was observed[6,15]. Due to the departmentalized structures of bio-media, nonlinear chemical waves of discrete systems [16-17] would be their closely related analogs. In the heart, fibrotic nonexcitable ''dead'' tissue normally is present at a small percentage of normal heart tissue. As a result of aging, after a myocardial infarction (heart attack), or in the case of cardiac myopathies, the percentage of fibrotic tissue increases dramatically, up to 30% to 40%[18-19]. Interesting observations showed that there is a wave-form change from planer wave to multiple spiral wavelets accompanying the procession from normal sinus rhythm to ventricular tachycardia, and finally to ventricular fibrillation[20] as shown in Figure 1.4.
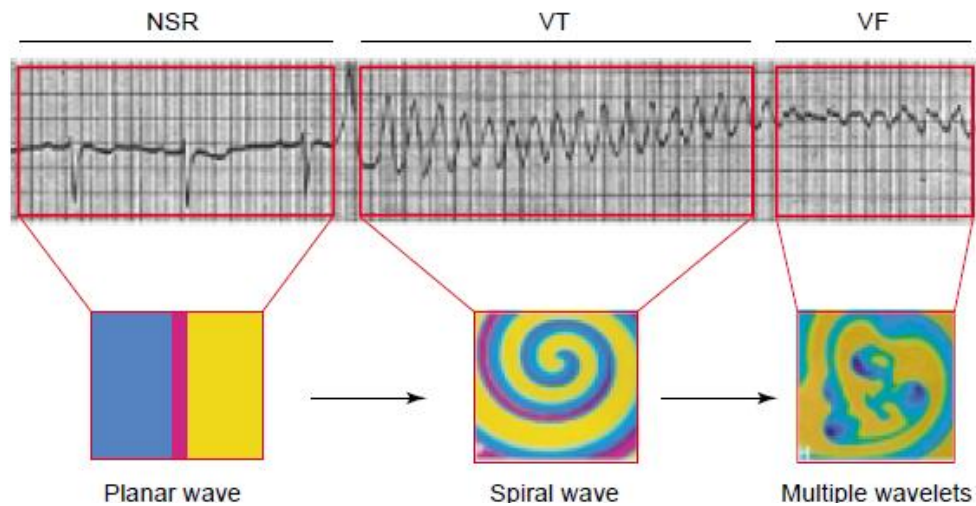
Figure 1.4 Proposed evolutions of cardiac wave propagation patterns. The evolutions were underlying the transition from a normal cardiac rhythm to ventricular fibrillation. Transition from normal sinus rhythm (NSR) to ventricular tachycardia (VT) and ventricular fibrillation (VF), as recorded on the surface electrocardiogram.[20]

Also, in a monolayer of chick embryonic heart cells, transition has been observed from target to spiral wavelets[21] as shown in Figure 1.5. Both transitions are caused by increased heterogeneity of the environment in which the wave patterns are generated and propagated. Insight into the dynamics of spirals in bio-excitable media and the understanding of the genesis of spiral waves and their interactions is vital to the development of effective approaches to interrupt arrhythmias.
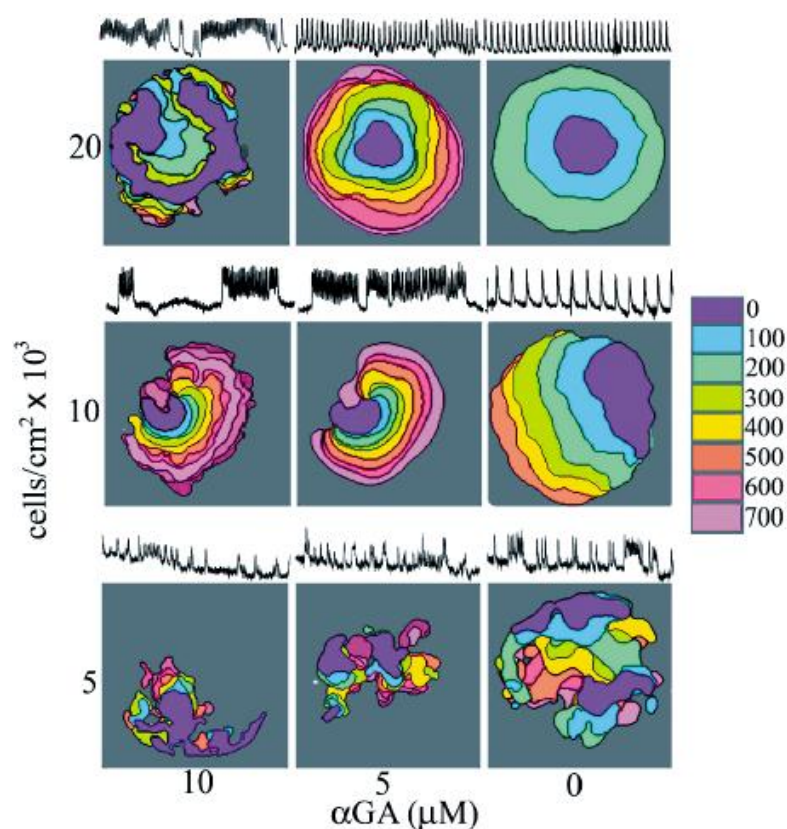
Figure 1.5 The activity of embryonic chick heart cell monolayers. Cells were plated at three different densities under different concentrations of gap junction blocker αGA visualized with calcium sensitive fluorescent dye.[15]

Scientists also developed a self-oscillating gel system by embedding BZ reaction into stimulus gels. They converted the chemical reaction to mechanical forces and induced dynamic swelling-shrinking behavior of the Poly (N-isopropylacrylamide) as shown in Figure 1.6.[22]
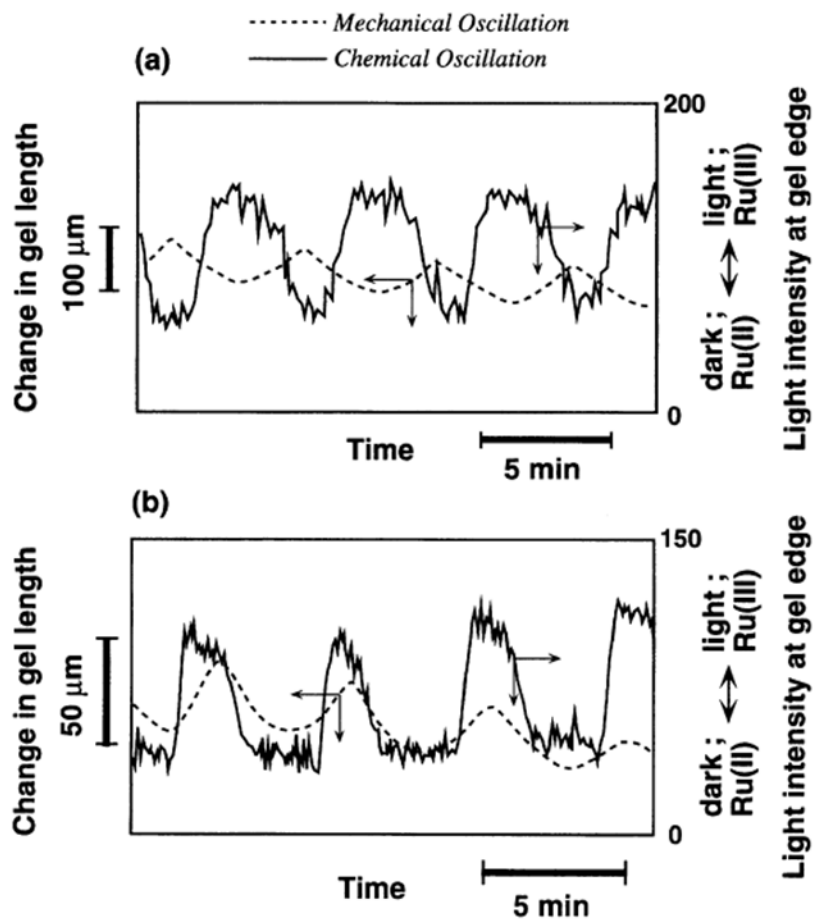
Figure 1.6 Periodic redox changes at the edge position of the rectangular gel and the swelling-shrinking oscillation.[22]

In this study (Chapter II), to mimic the "dead" cells conditions, first we immobilized the BZ catalyst in some ion exchange resin beads to create "live" cells.

Then by mixing "live" cells together with those fresh beads without the catalyst at various ratios, different levels of heterogeneities were achieved. Then various types of wave patterns were observed in the reactant solution. The key discovery was a transition from target wave patterns to spiral wave patterns. This model could be used to predict wave behaviors under similar conditions and display specific wave patterns under different requirements.

Periodical Polymer Drug Delivery System

Drug delivery is a hot topic in modern society. Even though many excellent drugs have been produced, the delivery process is not precise enough resulting in low efficiency. Traditional methods require several doses daily to maintain the drug level in plasma in the therapeutically effective region which is right under the toxic region. Thus, to develop a device that can automatically release the drugs encapsulated at a proper time with only one dose is vital to overcome the problems. "Smart" gels were utilized to develop new drug delivery vehicles. Smart gels are polymers that responsd to different stimuli. They switch between two phases (usually hydrophobic and hydrophilic) accompanied with changes of pH, temperature, ion strength and other factors[23-25]. Thus, we can design various devices to meet different requirements. They have many applications as drug delivery vehicles[26], biosensors[27], chemical separation and water purification agent[26,28]. As a drug delivery vehicle, smart gels may release the drugs periodically according to the drug level in the plasma. So drug level could be maintained in the therapeutically effective region and help the patient to recover much faster than

the traditional methods. A self-oscillating model has been built based on N-Isopropylacrylamide and Methacrylic acid[29] recently. Results showed that the membrane could periodically open and close using a proton generator and a proton consumer. There existed a time delay which could lead to a pH value change periodically. Their device is shown in Figure 1.7. With this method, they have achieved promising results that could be further utilized in clinical treatment as shown in Figure 1.8. The model can benefit those patients who has trouble to follow the traditional drug delivery methods or with chronic disease.
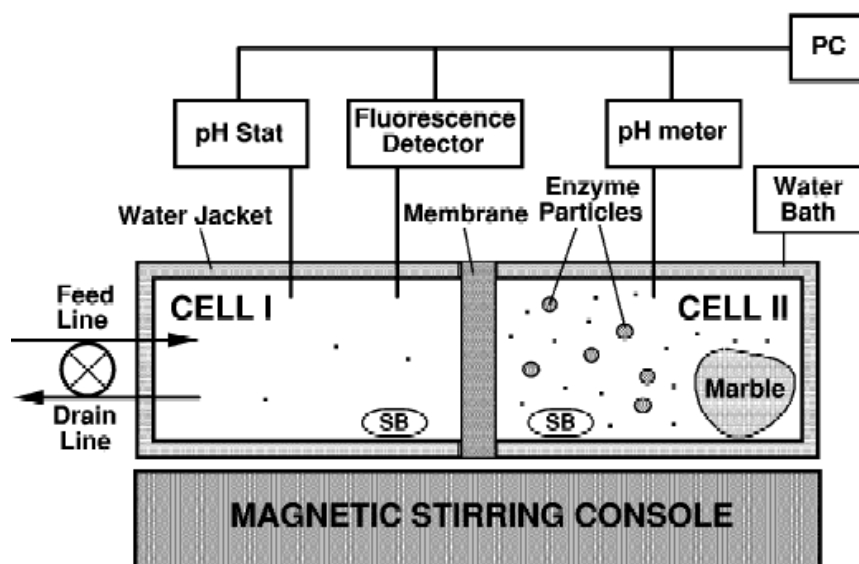
Figure 1.7 Diagram of test cell for delivery of GnRH. Both Cells I and II are charged with 75ml solutions, which are stirred vigorously at constant temperature.[29]
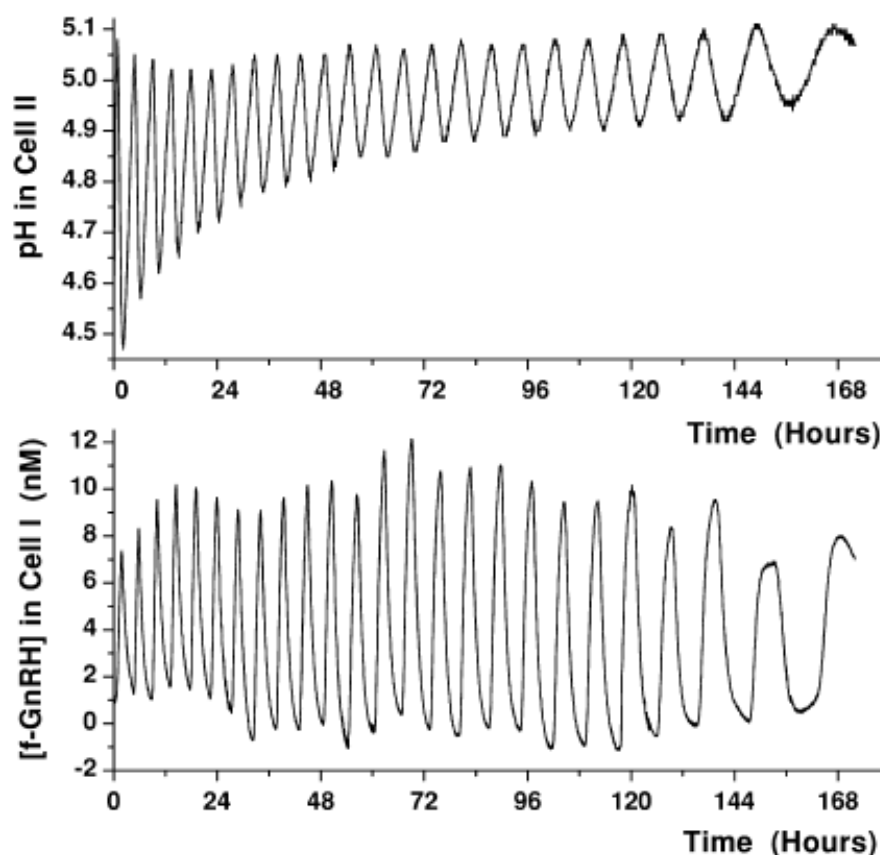
Figure 1.8 Time course of oscillations of pH and concentration of GnRH.[29]

In our research (Chapter III), we used a similar mechanism to construct a delivery vehicle but avoiding the use of marbles. Ion exchanger Zirconium Phosphate was embedded in the Poly(Acrylic Acid) matrix which is pH sensitive. Zirconium Phosphate was first developed by Dr. Abraham Clearfield[30]. It has the capability to undergo an ion exchange reaction with cations to produce protons. It is an inorganic nanoparticle with very high aspect ratio due to the layered structure of the crystal as shown in Figure 1.9. The hydrogen atom will lose its electron to the corresponding

oxygen atom in the hydroxyl group and become a proton after the ion exchange. Thus, we can use the sodium ions to control the behavior of the pH sensitive polymer matrix as shown in Figure 1.10. The original sample (status 1) swells to status 2 in a buffer environment by absorbing water. Then the permeability of sodium ions increases and ZrP generates protons to shrink the sample to status 3. The permeability of sodium ions decreased and the generation of protons slows down. Then the consuming of protons by the components of the buffer is faster and the gel swelled again to status 4. Then the same process happens again and again to form an oscillation. If medicines are encapsulated in the hydrogel, a periodical release can be realized.
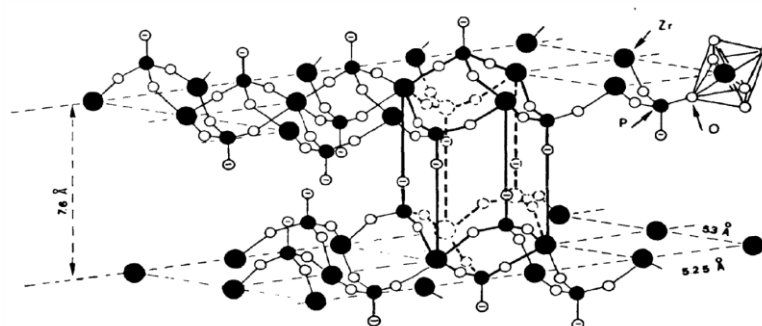
Figure 1.9 Layered structure of Zirconium Phosphate.[31]
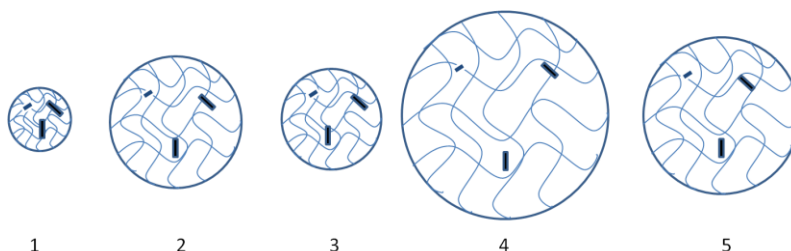
Figure 1.10 Schematic process of the oscillating swelling and shrinking behavior of pH sensitive gel embedded with ZrP.

CHAPTER II

EFFECTS OF HETEROGENEITY ON THE WAVE PATTERN FORMATION

A series of heterogeneous BZ reactions were carried out to investigate the effects of heterogeneity on the formation and propagation of the wave patterns. A transition from target wave pattern to spiral wave pattern was observed. The generation of spiral pairs and the process to develop into a single spiral pattern was observed. Three regions were established based on the types of wave patterns and their characteristics.

Experiment Set Up and Procedure

To introduce heterogeneities into the BZ reaction system, we need at least two different kinds of components. Thus, we choose to combine some fresh polystyrene ion exchange resin beads which is called inactive beads and same kind of beads but loaded with the catalyst, Ferroin, named active beads. The size of the beads was between 75 to 150μm. We immersed the fresh beads in a 0.025M (i.e., mol/L) Ferroin aqueous solution in a capped glass bottle in a dark environment to avoid the decomposition of Ferroin. The loading process lasted 10 hours to make sure there was no Ferroin left and the aqueous solution became colorless. Then the beads were filtered and dried overnight. The catalyst concentration in active beads was fixed at a constant of 25mol/g to avoid the difficulties of analysis brought by other heterogeneous factors. BZ reactants for all experiments were 50ml aqueous solutions of sulfuric acid (0.25 M), malonic acid (0.025 M), and sodium bromate (0.25 M).

In each experiment, a total of 10g of beads was used. The percentage of active beads ϕ was varied from 20% to 100%. Experiments were carried out in a beaker with a diameter of 9 cm. The thickness of beads was about 5mm and the depth of the reactants plus the beads was about 1.5 cm. To record the formation and propagation of different wave patterns, a camera was installed 1.5 m directly over the beaker and images were taken every 10 seconds in a dark room. The reaction temperature was maintained at 15 ℃ by a temperature controller. The whole set up is shown in Figure 2.1.
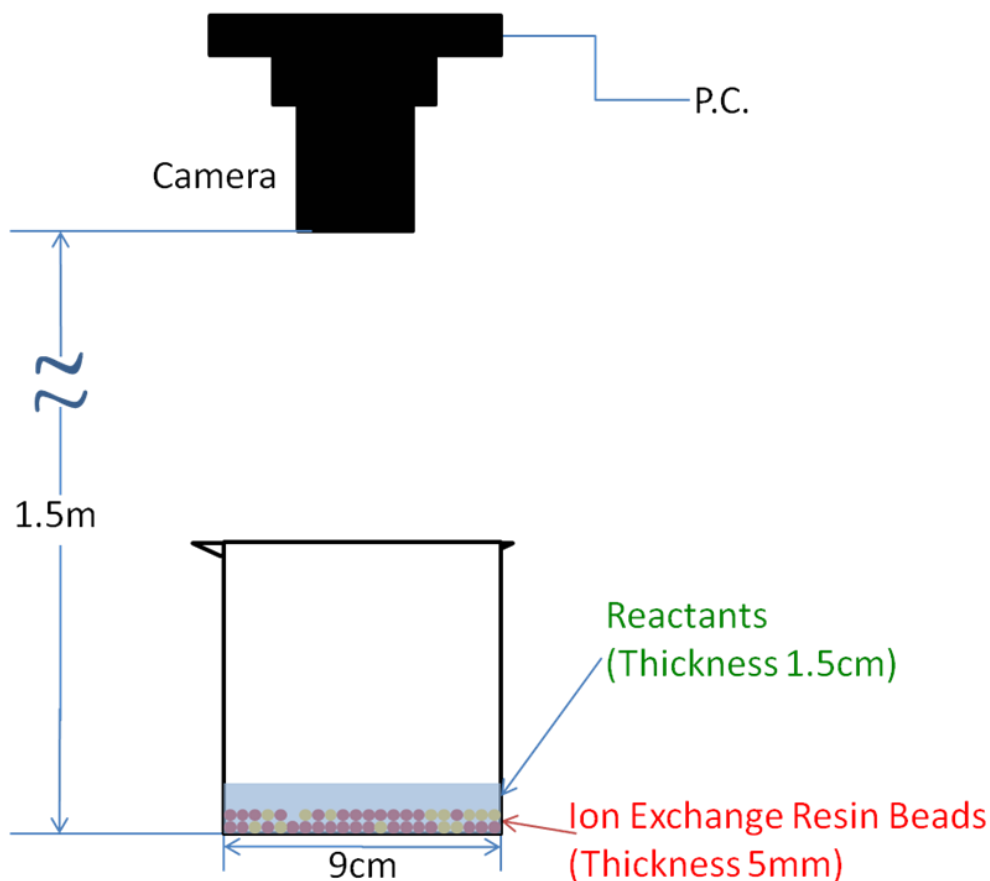
Figure 2.1 Set up to carry out and record the heterogeneous BZ reactions.

Formation and Propagation of Wave Patterns

BZ wave patterns were generated at various active bead percentage ϕ. The snapshots of the steady wave patterns are displayed in Figure 2.2. Target wave pattern dynamics were observed for $\phi \geq 0.7$. In the range of $0.5 \leq \phi \leq 0.6$, target waves were formed, but the wave crests close to the center are rough and the whole pattern became non-circular. For $\phi \leq 0.4$, multiple wave initiation sites and various wave patterns coexisted, and single rotating spirals were generated. Therefore, the composition of inactive resin beads (1- ϕ) acts as a dynamic bifurcation parameter. As ϕ decreases, steady state of the system made a transition from target to spiral separated by a transient region.

A special pattern was generated in one of the experiments at $\phi = 0.3$. Instead of multiple initiating sites and multi-waves, a wave pattern generated at the early stage by a high-frequency pacemaker occupied the whole area in this particular experiment. At the wave center, the wave crest appeared as a closed line but distorted into a shape different from a circle, as shown in Figure 2.3(a). The time sequence is shown in Figure 2.3(b). Due to the presence of the inactive beads, the continuity of the wave was destroyed and three separate pieces can be identified (insets of Figure 2.3(b)); these pieces grew into three wave segments while moving away from the center. The segments were intended to curve and grow into spiral pairs. However, the distance between the segments was so small that they quickly met and joined into a closed wave pattern which is different from the target waves.
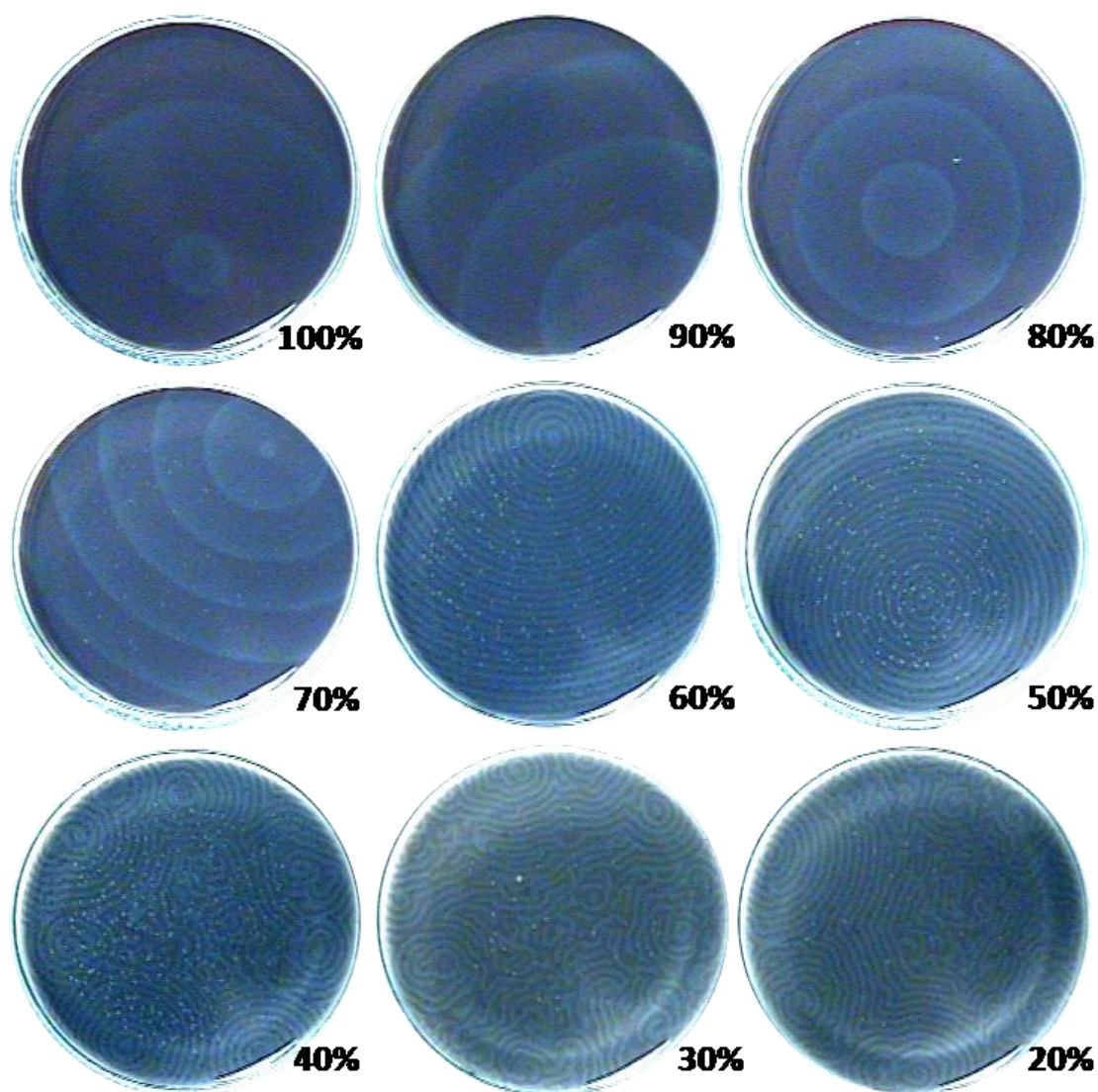
Figure 2.2 The BZ wave patterns change from target to spiral with the reduction of the number of active beads. The percentage of ferrion loaded resin beads are labeled in the right bottom corner. Image sizes are 9 cm.
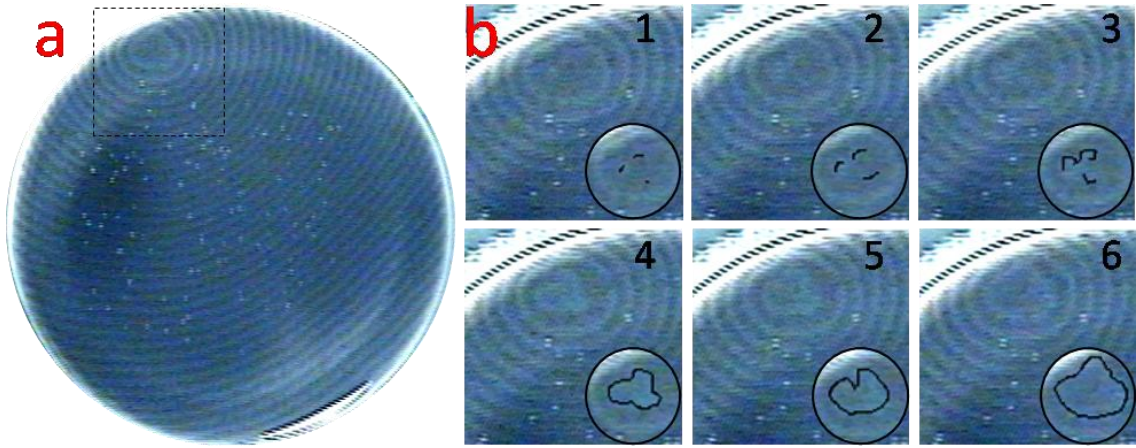
Figure 2.3 The closed wave pattern observed at $\phi = 0.3$. (a) The closed irregular wave pattern at the steady state with a pacemaker near the edge. (b) The process to generate the closed irregular pattern through the joint of three wave segments. The image sizes are about 2.9 cm. Time separation between sequential frames is 40 seconds. The insets illustrate the center of the wave.

Bound spiral pairs were observed for samples at $\phi = 0.2$, where the wave segments were further separated and allowed to become fully developed spiral waves as shown in Figure 2.4(a). Such states are metastable, however, as two spirals in one pair had opposite topological charges, so would likely repel[32-33]. The higher-frequency spiral in the pair could expand faster and take over the other spiral, as shown in Figure 2.4(a). The dynamics of spirals are also peculiar in the presence of inactive cell clusters, as shown in Figure 2.4(b). For a given period of the spiral rotation, the center of the single spiral first develops a closed geometric pattern composed up of wave segments. It

expands with upward growth. Then the closed pattern expands in the horizontal direction and forms a semicircle on the left half (Figure 2.4(b)-4). Meanwhile, it starts to rotate in the clockwise direction together with the whole spiral pattern (Figure 2.4(b) from 4 to 5), and the closed segments open up. Finally, the straight segment with a free end curves and rotates (Figure 2.4(b) 6 and 7), setting the stage for the next period.
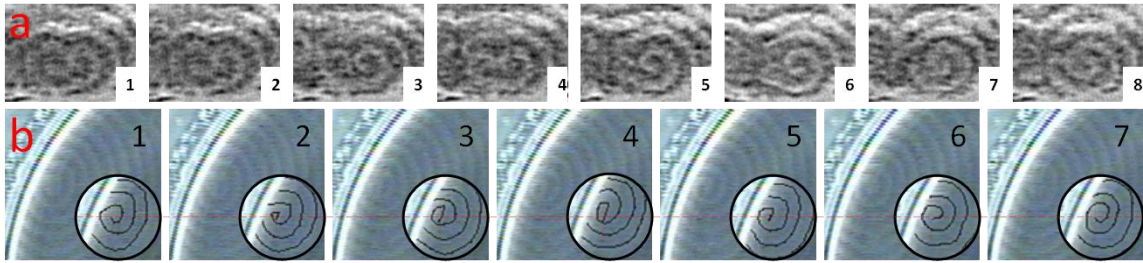
Figure 2.4. The spiral patterns at $\phi = 0.2$. (a) The process of generating a single spiral pattern from a spiral pair. The image sizes are about 1.65 cm in length. (b) Rotation of a single spiral. The time separation between sequential frames is 30 seconds. The image size is about 2.65 cm. Insets illustrate the center of the spiral wave. Frame 1 and 7 are the beginning and end of a spiral rotation period, respectively.

Mechanisms to Introduce the Wave Pattern Transition

When $\phi = 1$, every bead in the system is able to be excited so that the pattern was a perfect target pattern. When ϕ started to decrease, some of the beads were not able to involve in the BZ reaction and the propagation of the waves was affected. The waves were generated with shorter wavelength and higher frequency to overcome the change of

the beads composition which is consistent with theoretical predictions [34-35]. Thus we observed drop of the wavelength and quicker generation of wave patterns.

Right below ϕ=0.6, the percentage of inactive beads reached a critical value that made them form clusters of a large expanse that significantly hindered the wave propagation by functioning as obstacles [36-37] shown in Figure 2.5. The generation of the distorted pattern was also caused by the lateral instability[38]. Thus, distorted target patterns were observed in the beaker as shown in Figure 2.2 for ϕ=0.6 and 0.5. The wave crests closer to the center exhibited an unsmoothed edge and an eccentricity of about 0.6. The roughness disappeared as waves propagated away from the centers, with eccentricity decreasing to 0.3. Therefore, the discrete system steps into a new regime as ϕ reduces through 0.6, which we call it transient region.
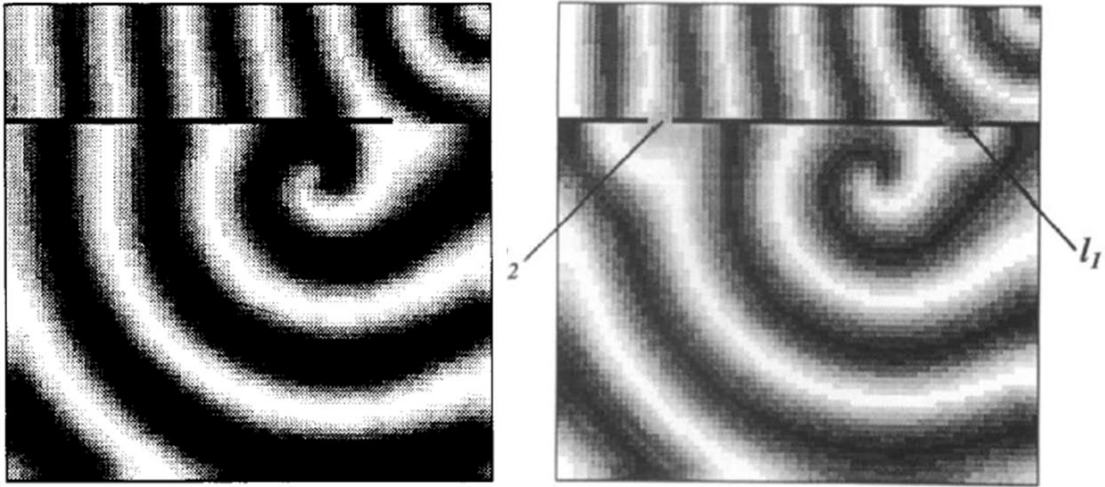
Figure 2.5 Formation of spiral wave patterns in the presence of obstacles.[36]

As ϕ decreased below 0.4, instead of only one pacemaker dominating, multiple initiation sites were generated, as shown in the bottom row of Figure 2.2. The new regime is called the spiral region. The formation of spiral pairs was starting from a short wave segment as previous theory hypothesized[39] shown in Figure 2.6. However, this also depended on the distance between the centers and that is why it only observed when $\phi =$ 0.2, which confirming the theoretical prediction[39-40].
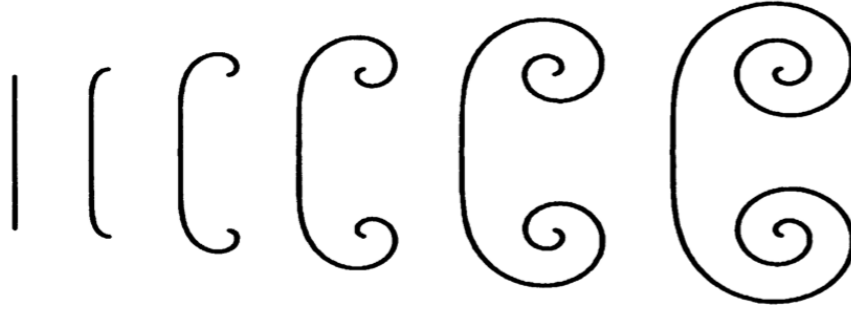
Figure 2.6 Time evolution of a straight front that has two free edges.[39]

Characteristics of Waves and Phase Diagram

Images captured from the camera were made into videos. Based on the videos, we made several calculations and found out some characteristics of the wave patterns as shown in Figure 2.7. In Figure 2.7(a), we defined three regions based on the wave patterns. They are target region, transient region and spiral region. And we can also see that the period of the waves kept decreasing until it reached the transient region. When ϕ was reduced from 1.0 to 0.7, the propagation velocity of the waves decreased linearly, as shown in Figure 2.7(b). Wave characteristics showed significant changes at $\phi \sim 0.6$

compared with the perfect target pattern $\phi > 0.7$. Then, we defined the lower boundary of the transient region to be $\phi_{lower} = 0.48 \pm 0.01$ by doing a nonlinear curve fitting in Figure 2.7(b). The measured dispersion curve (velocity versus period) is plotted in Figure 2.7(c), showing a decreasing wave period as propagation velocity decreases, which showed consistency with pervious theories[41-42]. Therefore, the inactive beads slow wave propagation speed and produce high frequency waves. Correspondingly, the wavelength decreases along with ϕ as shown in Figure 2.7(d). We defined the upper boundary for the transient region is $\phi_{upper} = 0.59 \pm 0.01$ by doing a linear fitting in Figure 2.5(d).
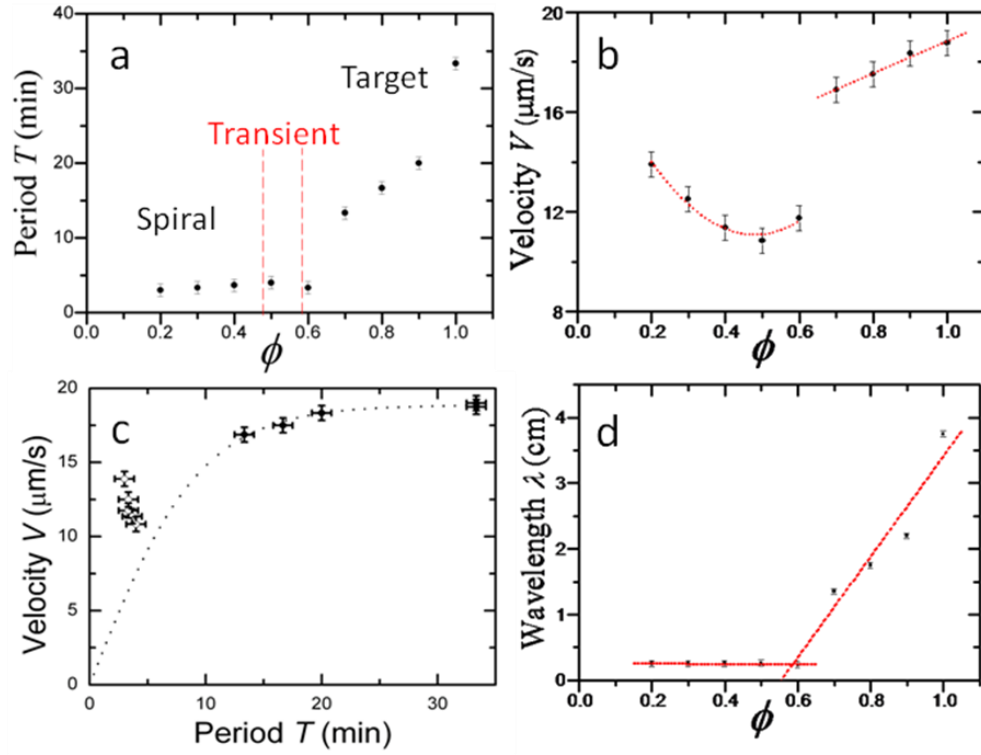
Figure 2.7 The characteristics of BZ waves vary with resin bead composition. (a) Period of the waves. Dashed lines indicate the boundaries of the target patterns to spiral patterns transition as ϕ decreases. (b) Propagation velocity of the waves. Dotted lines are the linear fitting to the data $\phi \geq 0.7$ and polynomial fitting to the data $\phi \leq 0.6$, respectively. (c) Dispersion of the BZ waves. The dashed curve is the fitting to the data $\phi \geq 0.7$ of $V = (18.87 \pm 0.12)*\tanh(T/(9.52 \pm 0.35))$. (d) Wavelength of the waves. The dotted lines are the linear fitting to the data $\phi \geq 0.7$ and $\phi \leq 0.6$, respectively.

CHAPTER III

FABRICATION OF DELIVERY SYSTEM WITH ZIRCONIUM PHOSPHATE

A novel self-controlled delivery vehicle was synthesized. The main components are pH sensitive polymer and proton generator. The hydrogel showed an oscillating volume change behavior at the beginning when immersed in a high pH solution. Later, the hydrogel shrank back when extra sodium chloride was added. The hydrogel also showed specific release behaviors when the amount of Zirconium Phosphate increases in a buffer solution.

Synthesis of pH Sensitive Polymer Containing Zirconium Phosphate

What we desired is a polymer network that will significantly change its volume when generation of a chemical species. So acrylic acid was chosen as the backbone of the polymer matrix since it has the highest ratio between the number of acid groups and the molecular weight of the monomer. We should be able to see the obvious volume change even with a small pH change. The change is purely due to the loss or gain of protons which simplifies the results. The poly (Acrylic Acid) will swell in high pH since its protons are consumed and the side groups are all negatively charged. The charged groups repel each other, and the volume and water permeability of the polymer increase. At low pH, the polymer shrinks because the side groups are not charged.

To build up the polymer matrix, we need crosslinkers to join the polymer chains together. Here we use the N,N'-Methylene bis(acrylamide) (BIS) as the crosslinker.

Although its amide structures is hydrophilic, we will ignore the effect since the amount of the crosslinkers is very small compare to monomers. An initiator was used to break the carbon-carbon double bonds and trigger the polymerization. We used the combination of Tetramethylethylenediamine and Ammonium persulfate to initiate the polymerization. They will generate free radicals and the reactions were carried out at about $60^{o}C$ to accelerate the process. To avoid the loss of water and acrylic acid, the reactions were carried out in an airtight bottle.

Acrylic Acid

N,N'-Methylene bis(acrylamide)

Tetramethylethylenediamine

Ammonium persulfate
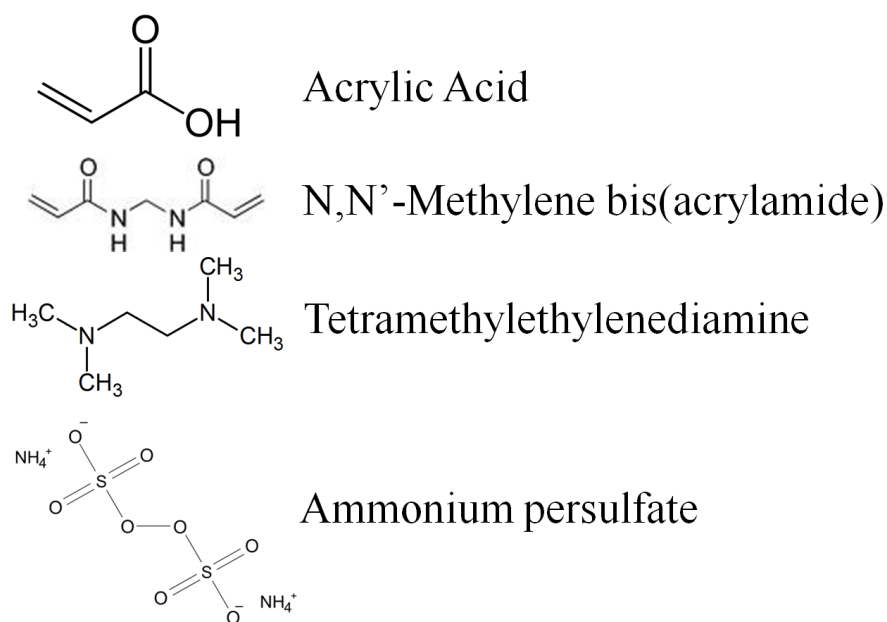
Figure 3.1 Structure of the polymer components.

Then Vitamin B2 was chosen as a model drug since it has a yellow color and could absorb light in a certain range due to its ring structure as shown in Figure 3.2. In each experiment, certain amount of Acrylic Acid, Zirconium Phosphate, Vitamin B2 and

other chemicals were well mixed with water with a certain ratio to polymerize a behavior-controlled pH sensitive hydrogel.
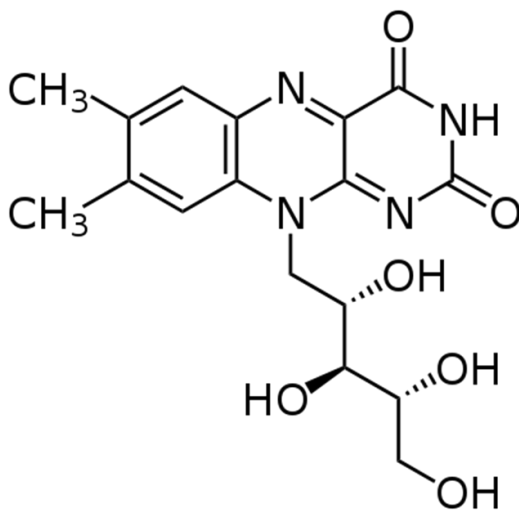
Figure 3.2 Structure of Vitamin B2 (Riboflavin).

Controlled Volume Change of Polymer Matrix Using an Ionic Exchanger

The very first experiment was to test the capability of ZrP to shrink the gel when it swelled in a high pH environment. After synthesis a chunk of the hydrogel, three identical small pieces were cut off from it. Then they were put into 100ml DI water. 100μl 1M NaOH solution and different volumes of 1M NaCl solution were added right after the samples were put in water. A fast camera (DFG/LC2, Imaging Source Europe GmbH) was set up right over the beaker to capture the size of the cut gels. A pH probe was immersed in the solution to record the pH change at various conditions. When they swelled to the limit, an equal amount of extra NaCl solution was added into the solution to trigger the gels to shrink. The results were displayed in Figure 3.3. The hydrogels all

swelled first to the limit and they shrink back to a smaller size after extra NaCl was added.
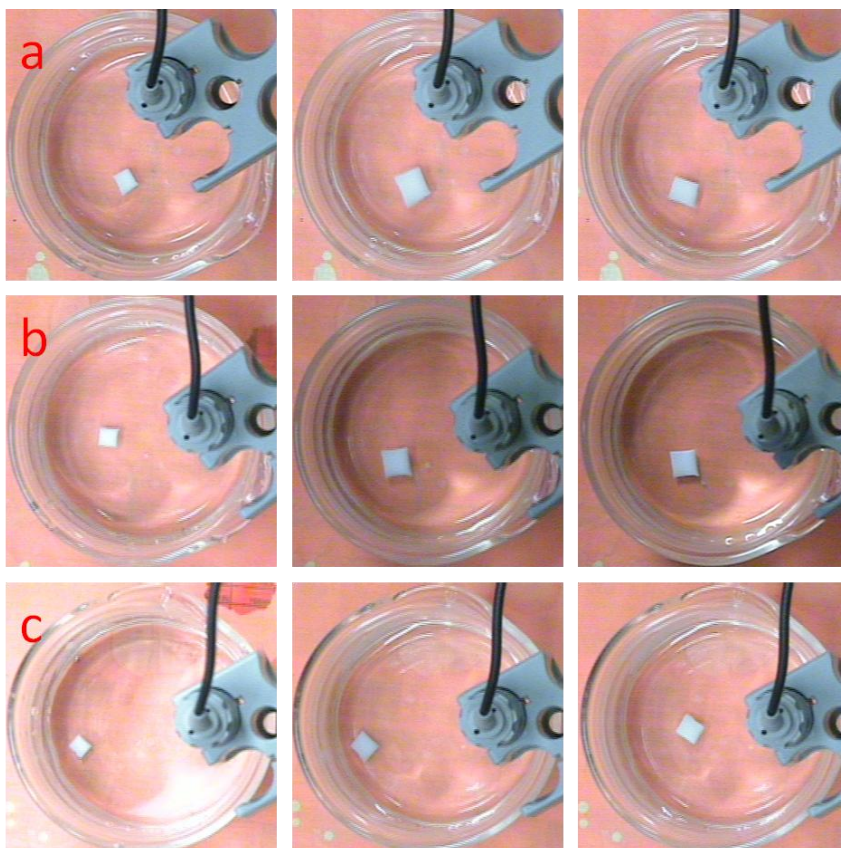
Figure 3.3 Swelling and shrinking behavior of pH sensitive hydrogel in various NaCl concentration solutions. Different volume of NaCl solution added into the whole environment from (a) 0ml, (b) 2ml to (c) 4ml, respectively. And in each row, the three pictures represented the status of the hydrogel from original, the swelling limit, and shrunk stage after extra NaCl was added.

Although the overall tendency was to absorb water and swell, the process was not that simple. So we measured the length of one side of the square shaped samples. Compared to the original side length, oscillation of the length was observed as shown in Figure 3.4. For the samples immersed in the least amount of NaCl, the side length kept increasing until it reached the limit. For the sample with 2ml NaCl solution, it shrank first with the help of ZrP and then swelled to a larger size. And then it shrank back again and swelled to an even larger size. The swelling behavior was then slowed down and finally reached to the limit. We fit the curve and to get the following equation:

$D_t/D_0 = (0.98 \pm 0.01) + (6.00E-7 \pm 8.93E-8) \times t + (2.58E-10 \pm 3.25E-11) \times t^2 + (-2.56E-15 \pm 3.22E-16) \times t^3$

$+ (0.022 \pm 0.035) \times \cos\{[(5.3E-4 \pm E-4) + (5.87E-10 \pm 2.84E-10) \times t] \times t\}$

And the fitting curve is shown in Figure 3.5. This oscillating volume change behavior is a very good confirmation of our hypothesis that there exists a non-equilibrium group of reactions which could control the behavior of the hydrogel automatically. With these reactions, we should be able to construct a novel drug delivery system which could achieve self-oscillating drug release behaviors in the near future. Next, several experiments were carried out to observe the drug release process from the hydrogel.
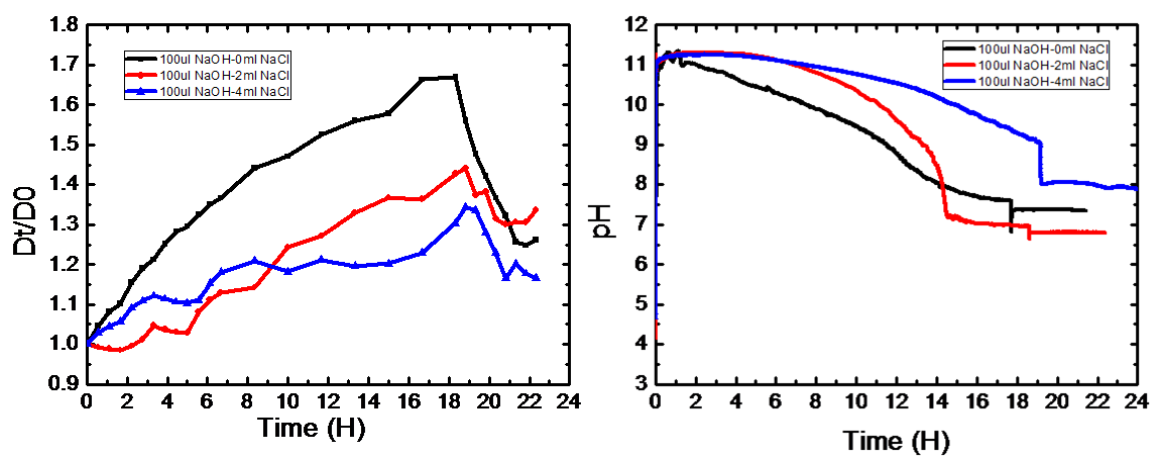
Figure 3.4 Swelling and shrinking behavior of PAA hydrogel controlled by various amount of Na$^+$ and the corresponding environmental pH value.
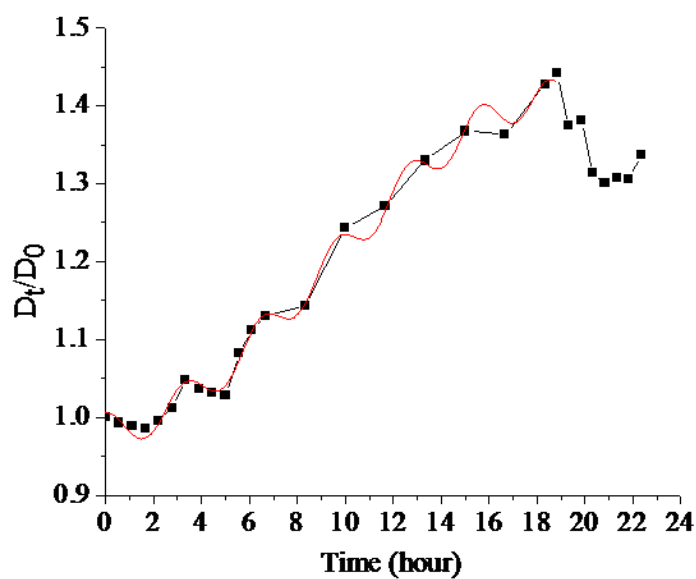

Figure 3.5 Fitting of the size oscillating behavior of a ZrP embedded hydrogel.

Drug Release Behavior from ZrP-PAA Composites

The size (volume) change only showed the potential capability of the system for drug delivery. There could be inhomogeneous expansion of the gel which has a large effect since we wanted to build up a drug delivery vehicle. So we designed the second series of experiments to observe the release behavior of the encapsulated chemicals (Vitamin B2) from the hydrogel. With these experiments, we can clearly find out what happens inside the hydrogel and if it is proper for drug delivery.

We have fabricated several disk-shaped hydrogels through the polymerization method mentioned above. They all had the same size in each series which made data comparison simple. The releasing environments were also the same. They were all kept in a buffer solution with sufficient amount of NaCl to assure the supply of Na^+. The pH value of the solutions was always kept high enough to drive the ion exchange reaction towards the direction of generating protons. The solution was kept homogeneous by using a magnetic stirrer all the time. Then solution samples were taken out at a certain time to measure the amount of Vitamin B2 released from the matrix using the UV-vis Spectroscope. It generated an absorption peak around 450nm and we have established a calibration curve to convert the absorption to the concentration of Vitamin B2 as shown in Figure 3.6. The red line is the fitting to the data points we have and the calibration formula is y= $(227.55 \pm 37.96)x^2 + (52.13 \pm 10.94)x + (0.62 \pm 0.07)$. With this calibration, we were able to generate the Vitamin B2 release curves with various types of gel and under various solution conditions.
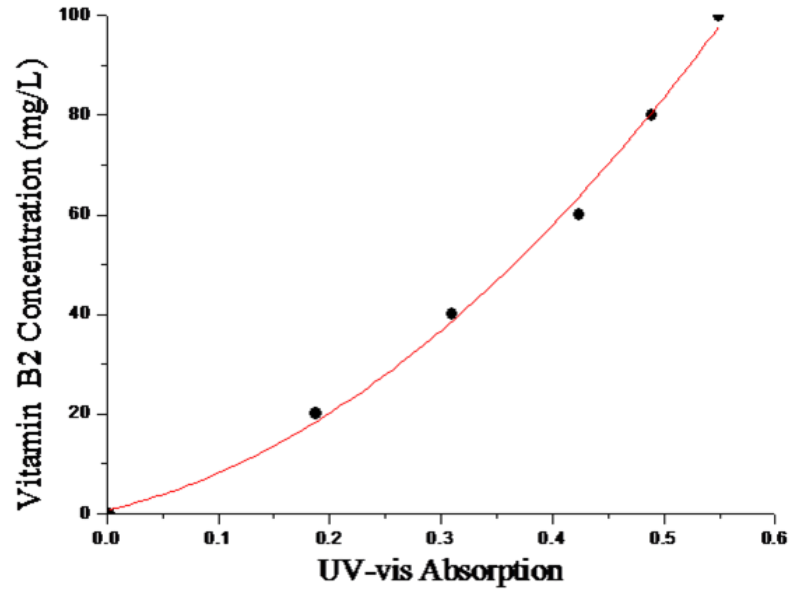
Figure 3.6 Calibration curve to convert the absorption at wavelength λ=450nm to Vitamin B2 concentration.

In the first drug release experiment, we prepared two samples, one with 0.03g ZrP and one without ZrP. The other compositions were the same and 0.04g Vitamin B2 was trapped in each sample. The samples were immersed in 100ml 1×PBS solution and kept stirring. Then by using the calibration curve, we obtained two curves as shown in Figure 3.7. The first hour release was very quick and slowed down since the concentration of Vitamin B2 of the outside environment was significantly increased. The sample containing ZrP released Vitamin B2 slower since the generation of protons inhibited the swelling of the hydrogel and lowered the permeability of Vitamin B2 and water. The lines are fitting curves giving $C = (45.1 \pm 3.7) \times t^{0.36 \pm 0.04}$ for the one without ZrP and $C = (24.4 \pm 1.0) \times t^{0.52 \pm 0.02}$ for the one embedded with ZrP. C is the concentration of Vitamin B2 and T is the time. The fitting was based on the theory model with a formula

$M_t/M_\infty=kt^n$.[43] M_t/M_∞ is the fractional solute release, M_t is the concentration of the encapsulated drug in the solution at time t and M_∞ is the concentration of the drug in the solution when the release time is infinite. Symbol t is the release time and k is a kinetic constant characteristic of the drug/polymer system. And n could be from 0.5 to larger values depended on what kind of diffusion model the sample follows. After differentiation, a new equation was obtained: $dM_i/Adt=nC_dkt^{n-1}$. M_i is the quantity of drug released at time t. C_d is the initial drug loading (soluble and insoluble) of the system.[44] For $n \leq 0.5$, the diffusion process is controlled is a by Fickian mechanism and the drug is molecularly dissolved in the polymer matrix. Case II: For n>0.5, it is an anomalous diffusion and the drugs are partially dissolved in the solution (i.e., it is loaded above its solubility limit). Thus the whole process contains the release/diffusion part and the dissolving part. Case III: For n=1, the diffusion is a limiting non-Fickian transport with the swelling agent front moves with constant velocity. Case IV: For n>1, systems exhibiting increased swelling at the relaxing front, usually at long periods of time.

Apparently, the hydrogel embedded with ZrP released the chemical slower than the pure gel since it has a smaller $(k \times M_\infty)$ value and the release rate decreased slower since it has a larger n value. This phenomenon is due to the presence of ZrP, that slowed down the swelling of the hydrogel since it produces protons through ion exchange with Na^+. The major effect of a small amount of ZrP on pH sensitive polymer is to slow down the release of the encapsulated drug with a more stable supply.
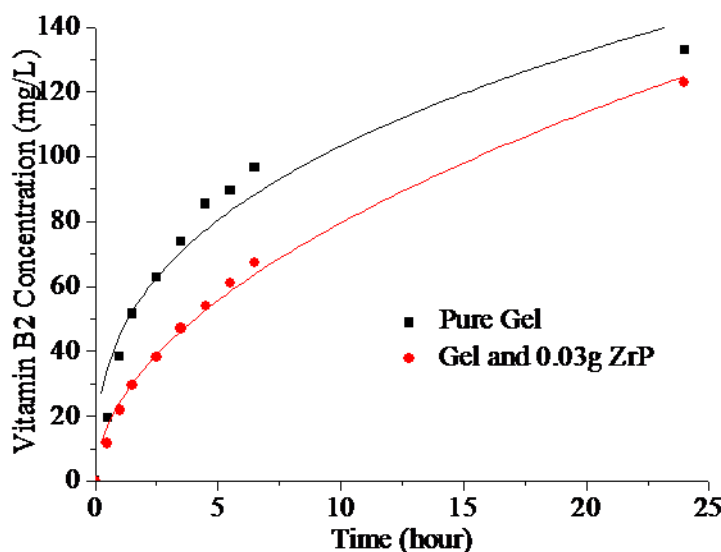
Figure 3.7 Drug release behavior of samples in $1\times$PBS solution.

Then three new hydrogel samples were synthesized with same components but different amounts of ZrP. To maintain the pH of the environment at a higher level to help the release of the encapsulated drug, a more concentrated PBS solution was used. The data was collected and converted into a curve shown in Figure 3.8. The hydrogel with 0.03g ZrP behaved similarly as the one without ZrP. And their fitting cuvre formulas are C= $(26.3\pm0.8)\times t^{0.57\pm0.02}$ for the pure hydrogel and C= $(17.5\pm0.6)\times t^{0.57\pm0.02}$ for the one with 0.03g ZrP. The release process of the sample with 0.12g ZrP had two steps. The first step is similar as the other two and the fitting curve formula is C=$16.5\times t^{0.48}$ (no errors obtained due to only three data points). The initial release for the large ZrP loading sample (0.12g ZrP) indicated more ZrP led to slower release and fast release rate reduction. We observed a second accelerated release of Vitamin B2 from the hydrogel. The fitting curve formula for the secondary release

C= $(14.1\pm4.9)+(22.7\pm5.6)\times(t-1)^{0.56\pm0.11}$. The fitting indicate that the secondary release was faster than the initial one (22.7>16.5) and the release rate reduction is slower (0.56>0.48) with the secondary release was similar to the release from the sample with lower ZrP loading (0.03g ZrP).
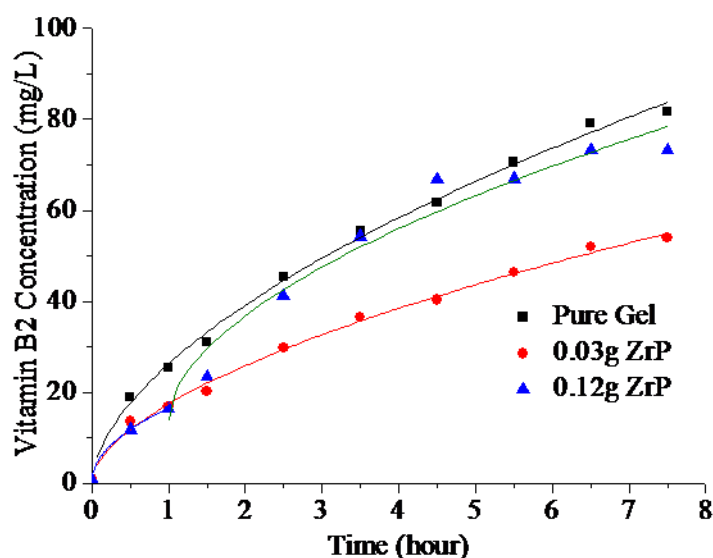
Figure 3.8 Drug release behavior of gel samples in 5×PBS solution.

To mimic the process of oral administration for the dried tablets, we established a series of experiments to investigate the release process of dried samples. Three samples were composed with same amount of all components but different ZrP amount. After synthesis, the samples were kept in an open cap bottle in the oven over night around 50°C. The hydrogels were thrown into the high concentrated PBS solution to observe the release behavior from a dry status. Results were shown in Figure 3.9. The sample with 0.06g ZrP released faster than the pure gel at the beginning because the ZrP might be

more hydrophilic than the polymer which gave the composite hygrogel a larger $(k \times M_\infty)$ value. The overall behavior can be fit into two curves with the formula $C=(36.1 \pm 1.9) \times t^{0.40 \pm 0.03}$ for the sample with 0.06g ZrP and $C=(18.1 \pm 0.6) \times t^{0.56 \pm 0.02}$ for the pure hydrogel. The release rate of the sample with 0.06g ZrP reduced faster than the sample without ZrP. The release from the hydrogel with 0.12g ZrP again showed a two stage release. In the initial release stage, the release rate was slower than the one with 0.06g ZrP and that is because the extra ZrP restricted the swelling of the hydrogel. It is very interesting to notice that the initial release had a constant release rate which indicated that the PBS buffer moved into the dried hydrogel at a constant speed (n=1).[43] The reason might be that was that at the beginning, unlike the other two samples, the higher amount of ZrP restricted the swelling of the hydrogel and reduced the loss of Vitamin B2 to the environment. Hence, the concentration difference of the amount of Vitamin B2 between the sample and environment was maintained. The secondary release of the dried sample behaved the same as the wet samples, a nonlinear release with a fitting curve formula $C= (34.5 \pm 1.1)+(18.7 \pm 1.2) \times (t-4)^{0.54 \pm 0.04}$.
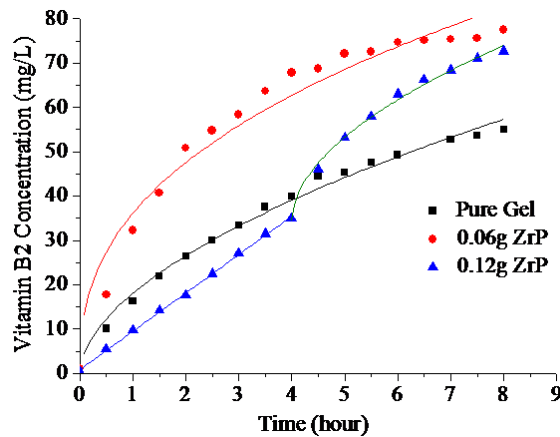
Figure 3.9 Drug release behavior of dried samples in $10 \times$PBS solution.

After investigating on the dried samples, to mimic a constant flow environment inside the human body, we kept changing the PBS solution every hour to observe the release behavior of the drug. The release amount of Vitamin B2 was first collected as shown in Figure 3.10(a). After adding up, we obtained the release profile as shown in Figure 3.10(b). It was remarkable that the secondary release (T > 2hours) had a constant release rate. The process could be maintained even longer than 8 hours as shown in the figures because most encapsulated drugs were still being held in the composite hydrogel.
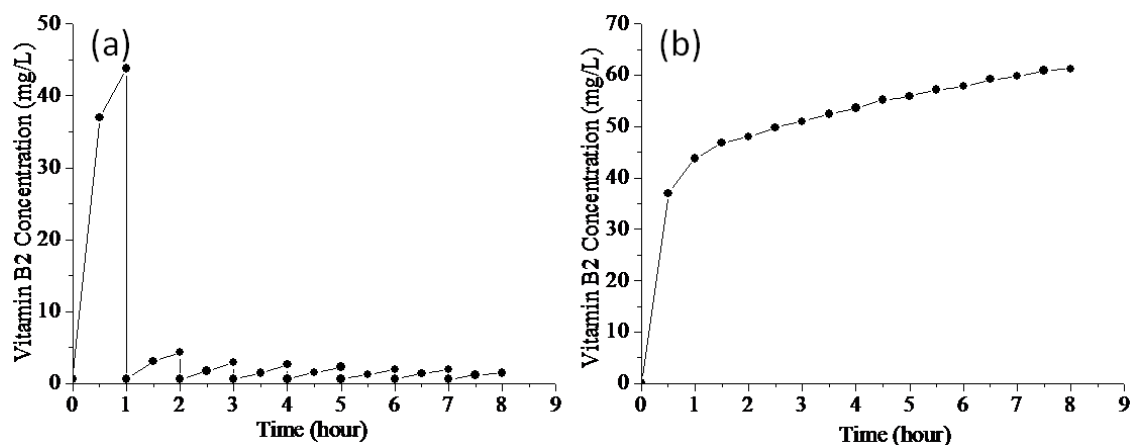
Figure 3.10 Release behavior of swollen sample in a quasi constant flow environment.

CHAPTER IV

CONCLUSIONS

Summary

Self-oscillating systems are of great interest and they could be found in many areas like in chemistry, physics and biology. It is so popular and important that it attracts a lot of attention in this particular area.

In **chapter II**, we have developed a model of discrete excitable media in which the population of inactive cells acts as the bifurcation parameter that controls the wave pattern transition from target to spiral. The behavior of bound spiral pairs and their separation indicates the scenario that the inactive clusters break the wave into segments and allow them grow into spiral pairs. This model system might be helpful to understand the occurrence of the spiral wavelets in the heart that cause the arrhythmias. It could also be utilized to discover methods to prevent and cure certain diseases.

In **chapter III**, based on a non-equilibrium behavior of a smart polymer, we have constructed a new drug delivery vehicle that could release drugs in a controlled behavior. The model showed the possibility to have a periodically swelling and shrinking behavior in a proper environment with the help of the ion exchanger Zirconium Phosphate. It also showed an interesting drug release behavior of multiple stages release and constant release. We were able to elongate the time of the constant release by modifying the ratio between the components. This method will increase the efficiency of medicine and get rid of some trouble in traditional drug delivery methods.

Future Projects

Wave generation based on monolayer uniform polystyrene beads

Although the transition from target wave to spiral wave was observed and well explained, there are still some problems needed to be solved. Our current system is a mixture of active and inactive beads and there were multiple layers. The interaction between layers is still not clear and it could really play an important role on the formation of wave patterns. Since it is really hard to observe the phenomenon directly, we will design a new series of experiments to set up a new system based on just one layer of the ion exchange resin beads. Thus the interaction could be clearly observed and it will be very helpful to fully understand the mechanism of wave formation.

Constructing periodically response drug delivery vehicle

We have achieved an oscillation volume change of the pH hydrogel by the help of Zirconium Phosphate in Figure 3.3. However, the drug release was still similar to prior results which exhibited a nonlinear release behavior. But we have seen a potential to achieve an oscillation since there were more than one release behavior during the release process as shown in Figure 3.8 and Figure 3.9. So the next series of experiments will focus on carrying out release in various conditions to find out the most suitable case to employ this technique. The composition of the hydrogel will also be changed to obtain various structures and properties of the polymer. Our technique will be able to be used not only as the drug delivery vehicle, but also as sensors, purification agents and packing agents.

REFERENCES

1   Bray, W. C. A periodic reaction in homogeneous solution and its relation to catalysis. *Journal of the American Chemical Society* **43**, 1262-1267 (1921).

2   Belousov, B. P. A periodic reaction and its mechanism. *Collection of Short Papers on Radiation Medicine*, **145** (1958).

3   Zhabotinsky, A. M. Periodic liquid phase reactions. *Proceedings of Academy of Science of USSR* **157**, 392-395 (1964).

4   Zaikin, A. N. & Zhabotinsky, A. M. Concentration wave propagation in two-dimensional liquid-phase self-oscillating system. *Nature* **225**, 535-537 (1970).

5   Zaikin, A. N. & Zhabotinsky, A. M. Propagation of concentration waves in a 2-demensional liquid-phase auto-oscillatory system. *Russian Journal of Physical Chemistry A,* **45**, 147 (1971).

6   Assenheimer, M. & Steinberg, V. Transition between spiral and target states in Rayleigh-Benard convection. *Nature* **367**, 345-347 (1994).

7   Davidenko, J. M., Pertsov, A. V., Salomonsz, R., Baxter, W. & Jalife, J. Stationary and drifting spiral waves of excitation in isolated cardiac-muscle. *Nature* **355**, 349-351 (1992).

8   Lechleiter, J., Girard, S., Peralta, E. & Clapham, D. Spiral calcium wave-propagation and annihilation in Xenopus laevis oocytes. *Science* **252**, 123-126 (1991).

9 Taylor, A. F., Tinsley, M. R., Wang, F., Huang, Z. & Showalter, K. Dynamical quorum sensing and synchronization in large populations of chemical oscillators. *Science* **323** (2009).

10 Mikhailov, A. S. & Showalter, K. Control of waves, patterns and turbulence in chemical systems. *Physics Reports-Review Section Phyiscs Lettters* **425**, 79-194 (2006).

11 Sagues, F. & Epstein, I. R. Nonlinear chemical dynamics. *Dalton Transctions*, 1201-1217 (2003).

12 Gorelova, N. A. & Bures, J. Spiral waves of spreading depression in the isolated chicken retina. *Journal of Neurobiology* **14**, 353-363 (1983).

13 Lechleiter, J., Girard, S., Peralta, E. & Clapham, D. Spiral calcium wave-propagation and annihilation in xenopus-laevis oocytes. *Science* **252**, 123-126 (1991).

14 Siegert, F. & Weijer, C. J. Analysis of optical-density wave-propagation and cell-movement in the cellular slime-mold dictyostelium-discoideum. *Physica D* **49**, 224-232 (1991).

15 Bub, G., Shrier, A. & Glass, L. Global organization of dynamics in oscillatory heterogeneous excitable media. *Physical Review Letters* **94**, 028105 (2005).

16 Greenberg, J. M. & Hastings, S. P. Spatial patterns for discrete models of diffusion in excitable media. *Siam Journal on Applied Mathematics.* **34**, 515-523 (1978).

17   Maselko, J., Reckley, J. S. & Showalter, K. Regular and irregular spatial patterns in an immobilized-catalyst Belousov-Zhabotinsky reaction. *Journal of Physical Chemistry* **93**, 2774-2780 (1989).

18   Ten Tusscher, K. & Panfilov, A. V. Influence of nonexcitable cells on spiral breakup in two-dimensional and three-dimensional excitable media. *Physical Review E* **68**, 062902 (2003).

19   Ten Tusscher, K. & Panfilov, A. V. Influence of diffuse fibrosis on wave propagation in human ventricular tissue. *Europace* **9**, 38-45 (2007).

20   Robert F. Gilmour, J. A novel approach to identifying antiarrhythmic drug targets. *Drug Discovery Today* **8**, 162-167 (2003).

21   Bub, G., Shrier, A. & Glass, L. Global organization of dynamics in oscillatory heterogeneous excitable media. *Physical Review Letters* **94**, 028105-028101-028104 (2005).

22   Yoshida, R., Yamaguchi, T. & Kokufuta, E. Molecular design of self-oscillating polymer gels and their dynamic swelling-deswelling behaviors. *Journal of Intelligent Material Systems and Structures* **10**, 451-457 (1999).

23   Chen, G. & Hoffman, A. S. Graft copolymers that exhibit temperature-induced phase transition over a wide rang of pH. *Nature* **373**, 49-52 (1995).

24   Peppasa, N. A., Buresa, P., Leobandunga, W. & Ichikawa, H. Hydrogels in pharmaceutical formulations. *European Journal of Pharmaceutics and Biopharmaceutics* **50**, 27-46 (2000).

25   Dahne, L., Leporatti, S., Donath, E. & Mohwald, H. Fabrication of micro reaction cages with tailored properties. *Journal of American Chemical Society* **123**, 5431-5436 (2001).

26   Galaev, I. Y. & Mattiasson, B. 'Smart' polymers and what they could do in biotechnology and medicine. *Trend in Biotechnology* **17**, 335-340 (1999).

27   Li, H., Yew, Y., Ng, T. & Lam, K. Meshless steady-state analysis of chemo-electro-mechanical coupling behavior of pH-sensitive hydrogel in buffered solution. *Journal of Electroanalytical Chemistry* **580**, 161-172 (2005).

28   Nath, N. & Chilkoti, A. Fabrication of a reversible protein array directly from cell lysate using a stimuli-responsive polypeptide. *Analyical Chemistry* **75**, 709-715 (2003).

29   Misra, G. P. & Siegel, R. A. New mode of drug delivery: Long term autonomous rhythmic hormone release across a hydrogel membrane. *Journal of Controlled Release* **81**, 1-6 (2002).

30   Clearfield, A. & Stynes, J. A. The preparation of crystalline zirconium phosphate and some observations on its ion exchange behaviour. *Journal of Inorganic and Nuclear Chemistry* **26**, 117-129 (1964).

31   Clearfield, A., et al., Mechanism of ion exchange in crystalline zirconium phosphates. I. sodium ion exchange of α-zirconium phosphate. *Journal of Physical Chemistry* **73**, 3424-3430 (1969).

32   Ruiz-Villarreal, M., Gomez-Gesteira, M., Souto, C., Munuzuri, A. P. & Perez-Villar, V. Long-term vortex interaction in active media. *Physical Review E* **54**, 2999-3002 (1996).

33   Xie, F., Qu, Z., Weiss, J. N. & Garfinkel, A. Coexistence of multiple spiral waves with independent frequencies in a heterogeneous excitable medium. *Physical Review E* **63**, 031901-031904 (2001).

34   Steinberg, B. E., Glass, L., Shrier, A. & Bub, G. The role of heterogeneities and intercellular coupling in wave propagation in cardiac tissue. *Philosophical Transactions of the Royal Society A* **364**, 1299-1311 (2006).

35   Alonso, S., Kapral, R. & Bar, M. Effective medium theory for reaction rates and diffusion coefficients of heterogeneous systems. *Physical Review Lettters* **102**, 238302 (2009).

36   Babloyant, A. & Sepulchre, J. A. Target and spiral waves in oscillatory media in the presence of obstacles. *Physica D* **49**, 52-60 (1991).

37   Sepulchre, J. A. & Babloyantz, A. Propagation of target waves in the presence of obstacles. *Physical Review Letters* **66**, 1314-1317 (1991).

38   Johnson, B. R., Scott, S. K. & Taylor, A. F. Reaction-diffusion waves-homogeneous and inhomogeneous effects. *Journal of the Chemical Society-Faraday Transactions* **93**, 3733-3736 (1997).

39   Meron, E. & Pelce, P. Model for spiral wave formation in excitable media. *Physical Review Letters* **60**, 1880-1883 (1988).

40   van der Deijl, G. B. M. & Panfilov, A. V. Formation of fast spirals on heterogeneities of an excitable medium. *Physical Review E* **78**, 012901-012904 (2008).

41   Flesselles, J.-M., Belmonte, A. & Gaspar, V. Dispersion relation for waves in the Belousov-Zhabotinsky reaction. *Journal of the Chemical Society-Faraday Transactions* **94**, 851-855 (1988).

42   Dockery, J. D., Keener, J. P. & Tyson, J. J. Dispersion of traveling waves in the Belousov-Zhanbotinskii reaction. *Physica D* **30**, 177-191 (1998).

43   Korsmqer, R. W., Gumy, R., Doelker, E., Buri, P. & Peppas, N. A. Mechanisms of solute release from porous hydrophilic polymers. *International Journal of Pharmaceutics* **15**, 25-35 (1983).

44   Langer, R. S. & Peppas, N. A. Present and future applications of biomaterials in controlled drug delivery systems. *Biomaterials* **2**, 201-214 (1981).

VITA

Guanqun Wang received his Bachelor of Science degree in biological sciences from The University of Science and Technology of China in 2006. He entered the Materials Science and Engineering program at Texas A&M University in August 2008 and received his Master of Science degree in May 2010. His research interests include understanding the mechanism of self-oscillating systems and its application.

Mr. Wang may be reached at the Department of Chemical Engineering, Texas A&M University, 3122 TAMU, College Station, TX 77843-3122 USA. His email address is Guanqun.Wang@chemail.tamu.edu.